Geochemistry, Geophysics, Geosystems

RESEARCH ARTICLE
10.1029/2018GC007654

Noble Gases in Deepwater Oils of the U.S. Gulf of Mexico

P. H. Barry[1,2], M. Lawson[3], W. P. Meurer[3], A. Cheng[1], and C. J. Ballentine[1]

[1]Department of Earth Sciences, University of Oxford, Oxford, UK, [2]Now at Marine Chemistry and Geochemistry Department, Woods Hole Oceanographic Institution, Woods Hole, MA, USA, [3]ExxonMobil Upstream Research Company, Houston, TX, USA

Key Points:
- Noble gas data are presented from two offshore oil fields
- Results are used to determine fluid migration pathways and the relative volumes of oil versus water in the subsurface
- This technique is robust for determining relative hydrocarbon values and could be used to determine large in-place hydrocarbon reservoirs

Correspondence to:
P. H. Barry,
pbarry@whoi.edu

Citation:
Barry, P. H., Lawson, M., Meurer, W. P., Cheng, A., & Ballentine, C. J. (2018). Noble gases in deepwater oils of the U.S. Gulf of Mexico. *Geochemistry, Geophysics, Geosystems*, *19*, 4218–4235. https://doi.org/10.1029/2018GC007654

Received 3 MAY 2018
Accepted 29 SEP 2018
Accepted article online 10 OCT 2018
Published online 5 NOV 2018

Abstract Hydrocarbon migration and emplacement processes remain underconstrained despite the vast potential economic value associated with oil and gas. Noble gases provide information about hydrocarbon generation, fluid migration pathways, reservoir conditions, and the relative volumes of oil versus water in the subsurface. Produced gas He-Ne-Ar-Kr-Xe data from two distinct oil fields in the Gulf of Mexico (Genesis and Hoover-Diana) are used to calibrate a model that takes into account both water-oil solubility exchange and subsequent gas cap formation. Reconstructed noble gas signatures in oils reflect simple (two-phase) oil-water exchange imparted during migration from the source rock to the trap, which are subsequently modified by gas cap formation at current reservoir conditions. Calculated, oil to water volume ratios ($\frac{V_o}{V_w}$) in Tertiary-sourced oils from the Hoover-Diana system are 2–3 times greater on average than those in the Jurassic sourced oils from the Genesis reservoirs. Higher $\frac{V_o}{V_w}$ in Hoover-Diana versus Genesis can be interpreted in two ways: either (1) the Hoover reservoir interval has 2–3 times more oil than any of the individual Genesis reservoirs, which is consistent with independent estimates of oil in place for the respective reservoirs, or (2) Genesis oils have experienced longer migration pathways than Hoover-Diana oils and thus have interacted with more water. The ability to determine a robust $\frac{V_o}{V_w}$, despite gas cap formation and possible gas cap loss, is extremely powerful. For example, when volumetric hydrocarbon ratios are combined with independent estimates of hydrocarbon migration distance and/or formation fluid volumes, this technique has the potential to differentiate between large and small oil accumulations.

1. Introduction

Petroleum systems are inherently complex crustal regimes. Exploration strategies require an understanding of temporal and spatial charge mechanisms, fluid migration pathways, and knowledge of the distribution of regional trapping structures. Thermal maturity and the timing of hydrocarbon expulsion from source rocks can be predicted using basin evolution models, but such models rely heavily on assumptions of linearity in deposition and subsidence rates over timescales that are tectonically driven and thus can only provide semiquantitative constraints on timing of generation. Further, migration analysis is complicated by the facts that (1) drilling rarely penetrates the deep stratigraphy that the hydrocarbons migrate through during initial expulsion and (2) present-day stratigraphic/tectonic structures are used to infer paleo-migration pathways responsible for the transport of fluids in sedimentary basins. These structures have evolved with time and according to tectonic constraints thus partially overprinting the fluid pathway record. Geochemical biomarkers can be used to identify source rock and/or maturity information from the analysis of hydrocarbon fluids and rocks, but there are few tools apart from noble gases that can be used to identify and quantify the physical controls on secondary migration processes, pathways, fluid interaction, and behavior.

Noble gases are chemically inert and represent a unique tool for understanding complex crustal systems. Unlike other hydrocarbon tracers, such as bulk compositions or isotopic signatures that may be modified by thermal, chemical, or biological processes, the noble gases do not partake in these processes. Instead, they record the history of fluid interaction and emplacement, and thus provide limits on the volume of differently sourced fluids, which may have contributed to any particular system. Terrestrial reservoirs (i.e., air-derived, crustal, and mantle) have diagnostic noble gas isotopic compositions, and therefore, fluids derived from each reservoir can be readily identified. For example, isotopic and abundance compositions of various fluid sources in sedimentary basins can be used to identify and quantify physical exchange mechanisms between water, oil, and gas phases in a hydrocarbon system (Ballentine et al., 2002; Barry et al., 2016, 2017; Bosch & Mazor, 1988; Prinzhofer, 2013; Zartman et al., 1961). In air-saturated water (ASW), noble gases are dissolved at solubility equilibrium. In shallow aquifers, ASW represents the transport mechanism for air-derived

noble gases into the deeper subsurface. The distinctive *air-like* noble gas isotopic composition is preserved in ASW, whereas relative elemental compositions are modified by the differential solubility of the noble gases during recharge or burial (e.g., Ballentine & Hall, 1999; Kipfer et al., 2002).

Contact between groundwater and a subsurface oil phase results in noble gas partitioning (i.e., the proportional distribution between the phases) of the air-derived noble gases originally in the water phase. If phase separation occurs and a gas exsolves from oil to form a gas cap in a hydrocarbon accumulation, the noble gases will be further partitioned between the oil and gas phase. Such a scenario could arise as a result of changes in pressure-volume-temperature (PVT) conditions of the reservoir or from the addition of gas to oil driving it above the saturation pressure/first droplet point. The resulting noble gas composition of each phase is controlled by the thermodynamic conditions of the system and the extent of contact between the various phases. This process preserves a record of subsurface fluid phase interaction (oil-water, gas-oil), which can be used to understand the migration history and storage of the hydrocarbon phase (Aeschbach-Hertig & Solomon, 2013; Ballentine et al., 1991, 1996; Bosch & Mazor, 1988; Byrne et al., 2017, 2018; Darrah et al., 2015; Hiyagon & Kennedy, 1992; Gilfillan et al., 2008, 2009; Pinti & Marty, 1995; Torgersen & Kennedy, 1999; Zhou et al., 2005, 2012).

Radiogenic noble gas isotopes (e.g., ^{4}He and ^{40}Ar) are continuously produced in the Earth's crust by decay of radioelements U, Th, and K and can thus provide temporal constraints and isolation ages for fluids. The concentration of radiogenic nuclides can be predicted by estimating flux rates in open fluid systems (Castro, Goblet, et al., 1998; Castro, Jambon, et al., 1998; Torgersen, 2010; Torgersen & Clarke, 1985; Torgersen & Ivey, 1985; Zhou & Ballentine, 2006). In contrast, in closed systems where fluids are trapped and stored over geologic timescales, the rate of accumulation is critical for calculating isolation estimates (Ballentine et al., 2002; Barry et al., 2017; Cook et al., 1996; Holland et al., 2013; Solomon et al., 1996; Tolstikhin et al., 1996, 2017; Warr et al., 2018). In such closed systems, parent radionuclide concentrations in reservoir rocks are critical, as is the efficiency of release (Barry et al., 2015, 2017; Darrah et al., 2014; Hunt et al., 2012; Lowenstern et al., 2014; Tolstikhin et al., 2010, 2017) from the source rock into the fluid phase.

In this study, we present noble gas isotope and abundance data as well as major gas compositional and isotopic data from two oil-bearing basins in the U.S. Gulf of Mexico (GOM)-the Genesis and Hoover-Diana minibasins (Figure 1). The Genesis and Hoover-Diana fields are geographically, volumetrically, and geochemically distinct. In addition, the reservoir fluid phase varies from oil with associated gas in the Genesis, Hoover, and Madison fields to dominantly gas with a small underlying oil phase in the Diana field. We adapt a series of solubility models that were developed to understand two-phase (gas-water) systems (Barry et al., 2016, 2017) and two-phase oil systems in order to interpret three phase (gas-oil-water) systems. These models describe how noble gas concentrations and elemental ratios evolve as (1) ASW interacts with oil and (2) oil reaches gas saturation and forms a gas phase in the subsurface reservoir. We use air-derived noble gas isotopes in our models to determine the extent of exchange between oil and formation waters in these minibasins. Using this approach, we are able to assess the utility of noble gases in determining the migration history of oil and any subsequent phase partitioning in crustal systems.

2. Geological Background

2.1. Hoover-Diana

The Hoover-Diana salt-withdrawal minibasin is located approximately 260 km east of Houston, Texas, in the Alaminos Canyon and East Breaks areas of the U.S. GOM (Figure 1) at water depths of approximately 1,400 m. The minibasin initially contained six producing fields (Hoover, Madison, Marshall, Rockefeller, Diana, and South Diana). Samples for this study were available from the Hoover, Madison, and South Diana fields, respectively. The Hoover and Madison fields are located in the east of the minibasin and are dominantly composed of oil with the potential for small overlying gas caps. In contrast, the South Diana field is located in the west of the minibasin and is primarily composed of gas with the potential for a small oil leg at the base of the gas column. The presence of both gas and oil phases suggests that gas may have been lost from the South Diana trap via capillary leakage through the overlying seal (Sales, 1997). The eastern and western sides of the minibasin are separated by a shale diapir. Hydrocarbons from Hoover and Madison are hosted in a single Upper Pliocene reservoir interval (P1:10), whereas South Diana is hosted in

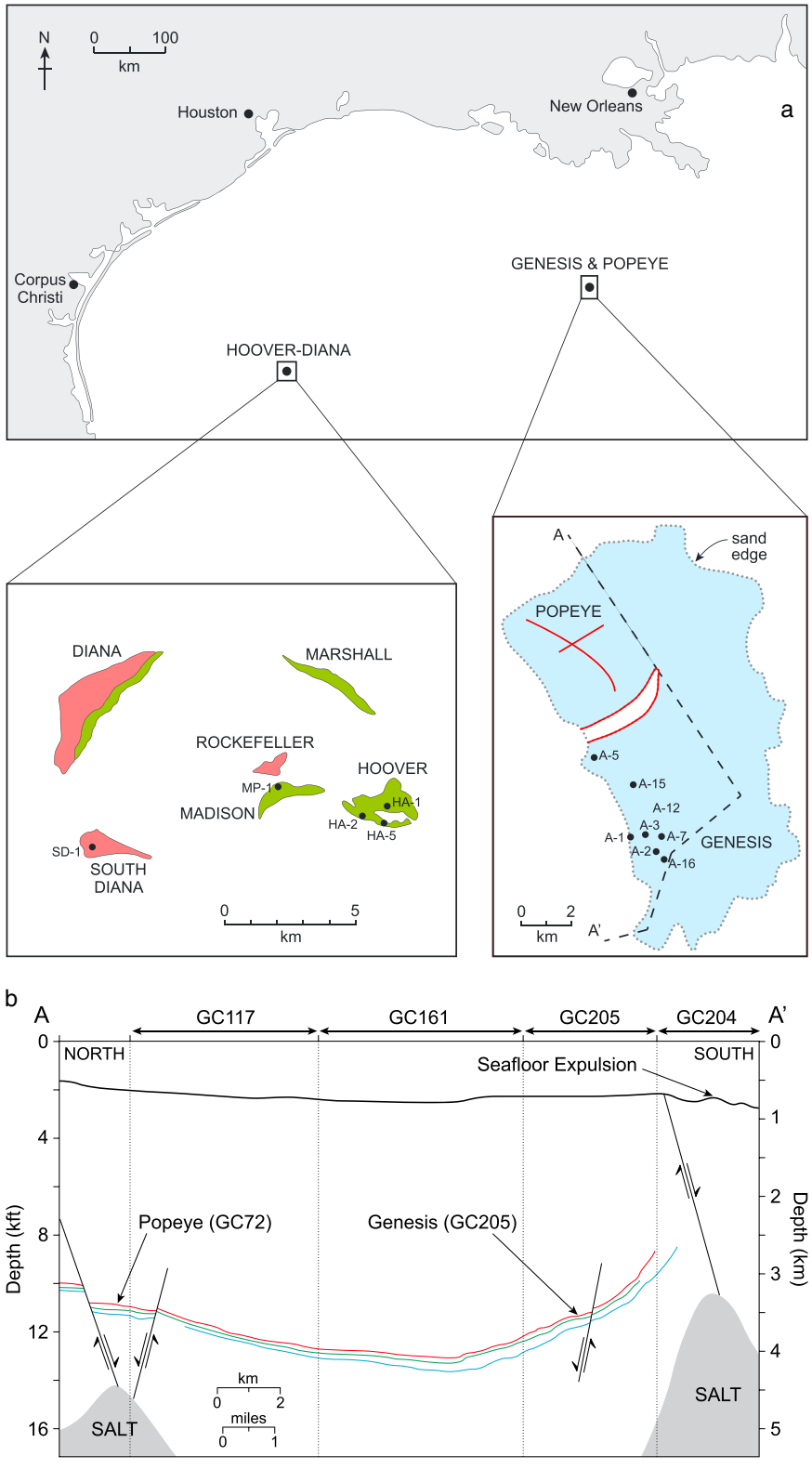

Figure 1. (a) Map view of the sampling region in the Gulf of Mexico, showing field boundaries for the Hoover-Diana and Genesis Oil Fields. Inset maps show the relative location of offshore wells in their respective reservoir. The Hoover-Diana basin hosts hydrocarbons in several single reservoir intervals, whereas hydrocarbons in the Genesis field are hosted in five stacked reservoir systems from the Pliocene and early Pleistocene. The red lines represent major faults in the Genesis mini basin. (b) Cross section A-A′ across the Popeye and Genesis field.

the A-50 reservoir. The P1:10 reservoir has been interpreted as a deepwater channel complex (Sullivan & Templet, 2002), while the A-50 sand is a composite of channel-axis, channel-margin, and interchannel facies, deposited in a relatively distal portion of a turbidite flow. Hydrocarbons in the minibasin are trapped in low-relief anticlinal structures, updip stratigraphic pinch-outs, and high-side three-way fault traps. The reservoirs have a range in depths from 1,914 m submud at South Diana to 2,441 m submud at Hoover. This gives rise to a range in reservoir temperatures from approximately 55–69 °C. The formation water at Hoover-Diana has a salinity of 3.026 M NaCl, likely as a result of the contact with the salt structures that are characteristic of this region of the GOM.

The hydrocarbons in the Hoover-Diana minibasin are generated from Tertiary marine-clastic source rocks (Hood et al., 2002). Maturation of the source rock was driven by late Tertiary deposition in the western GOM (Galloway et al., 2000), and hydrocarbons charged the Upper Pliocene reservoirs in the last 3 Ma following deposition. The inferred migration pathways in the Hoover, Madison, and South Diana fields are from the south and are presumed to be shorter (versus Genesis) based on biomarker data constraints on the likely source age and seismic constraints on the likely depth to this interval within the minibasin.

2.2. Genesis

The Genesis Field is located in the Green Canyon area of the central GOM in approximately 790 m of water. The field lies on the eastern flank of a salt-cored ridge that defines the western margin of the Popeye-Genesis Mini-basin. The Popeye Field lies on the northwest flank of this ridge, while Genesis is in the southwest (Figure 1). The ascension of the diapiric salt ridge governed the sedimentary processes and deposition and hence the reservoir distribution and geometry within the minibasin. These relationships are described in the larger Green Canyon area by Rowan and Weimer (1998). In contrast to the Hoover-Diana basin that hosts hydrocarbons in single reservoir intervals, hydrocarbons at Genesis are hosted in a faulted three-way trap against a salt diapir and produced from five major sands in a stacked Nebraska reservoir system that includes late Pliocene 14,800′, 14,500′, 14,200′ through early Pleistocene (Neb 3, Neb 2, and Neb 1) deepwater channel-fill and channel-levee reservoirs (Rafalowski et al., 1994; Sweet & Sumpter, 2007).

The oils at the Genesis field were generated from an Upper Jurassic carbonate influenced source rock (Hood et al., 2002). As with the Hoover-Diana system, the Genesis hydrocarbons must have charged the reservoirs in the last 3 Ma, given that the reservoirs are Upper Pliocene to Pleistocene age. The reservoirs are all over pressured, with initial pressures ~2,300 PSI above hydrostatic, and the leak mechanism is inferred to be pressure-induced fracture dilation in the capping mud units (Seldon & Flemings, 2005). The migration of hydrocarbons into the Genesis field requires a longer vertical pathway than those in the Hoover-Diana given the greater depth to the older Upper Jurassic source rock that generated the oils at Genesis (i.e., law of superposition and biomarker data); however, the length of the horizontal migration pathway is unclear. It is possible that hydrocarbons migrated along the salt diapir and charged top-down into the reservoirs. Alternatively, it is possible that hydrocarbons migrated laterally from near the center of the minibasin. This combined vertical and lateral migration pathway at Genesis is most likely significantly longer than that at Hoover-Diana due to the law of superposition and biomarker data.

Previous work reports on preproduction PVT samples suggested that oils from the Genesis field were undersaturated black oils with API gravities of 25–31° and 800–1,600 scf/stb solution gas oil ratios (Pourciau et al., 2003). The compositionally distinct oils in different reservoir intervals have been interpreted to reflect distinct charge events (Pourciau et al., 2003) but could also be related to differing extents of biodegradation.

The Pleistocene Neb 1 reservoir has a temperature range over the Pleistocene reservoirs from approximately 63 to 72 °C, and we use an average value of 68 °C for modeling purposes. In contrast, the Pliocene reservoirs (Neb 2 and 3) exhibit a temperature range from approximately 75 to 82 °C, and we use an average value of 79 °C for modeling purposes. Formation water salinity in the Genesis reservoirs is approximately 3.56 M NaCl. The producing intervals are separated from each other by muddy intervals that essentially preclude significant vertical connectivity (see cross section in Sweet & Sumpter, 2007). The pressure increases from the Neb 1 to the 14,500′ reservoir such that the Neb 1 has the lowest pressure (8,100–8,250 PSI), Neb 3 (8,100–8,400 PSI), 14,200′ (7,900–8,900 PSI), and the 14,500′ reservoir has the highest pressure (8,850–9,050 PSI).

3. Methods

3.1. Sample Collection

In 2014 (n = 5) samples were collected from the test separator on the Hoover-Diana minibasin platforms: three from the Hoover field, one from the adjacent Madison field, and one from the South Diana field. All Hoover and Madison samples are produced from reservoirs that dominantly contain oil, and the gas samples collected are *separator solution gases* that have been exsolved due to decompression during production. In contrast, the South Diana sample is gas phase in the reservoir, although the sample was also collected at the test separator on the platform.

In 2015 (n = 8) samples were collected from the Genesis minibasin platform, also from the test separator. The dominant fluid phase in the Genesis reservoirs is oil, and gas is exsolved at atmospheric pressure and temperature conditions, although gas is initially dissolved in oil at reservoir pressure and temperature.

Gases from each well location were collected in three industry standard 300 cc stainless steel (SS) cylinders that were individually leak tested on a vacuum line to minimize any potential contamination. One cylinder from each Genesis well was shipped to GeoMark Research LTD for analysis of stable isotopes and a complete suite of hydrocarbon gas compositions. Similarly, one cylinder from each Hoover-Diana sample site was shipped to Isotech for analysis of stable isotopes and a complete suite of hydrocarbon gas compositions. The remaining cylinders were shipped to the University of Oxford for noble gas analysis.

3.2. Analytical Techniques

Noble gas analysis was conducted in the Noble Laboratory at the University of Oxford, UK, using a dual mass spectrometer setup, interfaced to a dedicated hydrocarbon extraction and purification system. Gases were decanted from SS cylinders and subsampled in Cu-tubes, using an off-line vacuum transfer line. The subsample was then transferred to the extraction and purification line where hydrocarbons were reacted out by exposing gases to a titanium sponge held at 950 °C. The titanium sponge was cooled for 15 min to room temperature before gases were expanded to a dual hot (SAES GP-50) and cold (SAES NP-10) getter system, held at 250 °C and room temperature, respectively. A small aliquot of gas was segregated for preliminary analysis on a Hiden Analytical HAL-200 quadrupole mass spectrometer. All noble gas were then concentrated using a series of cryogenic traps; heavy noble gases (Ar-Kr-Xe) were frozen down at 15 K on an all SS finger and the He and Ne were frozen down at 19 K on a cold finger filled with charcoal. The temperature on the charcoal finger was then raised to 34 K to release only He, which was inlet into a Helix SFT mass spectrometer. Following He analysis, the temperature on the charcoal cryogenic trap was raised to 90 K to release Ne, which was inlet into an ARGUS VI mass spectrometer. Following analysis of Ne, the SS cryogenic trap temperature was raised to 200 K and an aliquot of Ar was inlet into the ARGUS VI to measure isotopes and total abundances. The remaining heavy noble gases (Kr-Xe) were then refrozen down on the SS cryogenic trap at 52 K and isolated, while any residual argon was pumped away from the manifold. The process of heating to 200 K, followed by cooling to 52 K, cryogenic isolation, and pumping of Ar was repeated a total of three times. After the third and final cycle, the Kr and Xe were simultaneously inlet into the ARGUS VI for simultaneous determination of Kr and Xe isotopic and absolute abundances.

4. Results

4.1. Major Volatiles and Stable Isotopes

Genesis major gases (n = 8) are composed of hydrocarbons (84–89% C1, 4–8% C2, and 3–4% C3), CO_2 (0.2–0.4%), and N_2 (0.2–0.3%); compositions are given in Table 1. Hoover-Diana major gases (n = 5) are composed of hydrocarbons (89–92% C1, 4–5% C2, and 2–4% C3), CO_2 (<0.13%), and N_2 (0.2–2.4%); compositions are given in Table 1.

4.2. Noble Gases

Genesis samples (n = 8) have relatively consistent noble gas concentrations, whereas Hoover-Diana samples show more pronounced variability. All Genesis noble gas isotope ratios (He, Ne, Ar, Kr, and Xe) are distinct from air, whereas the heavy noble gases (Ar, Kr, and Xe) from Hoover-Diana are indistinguishable from air-like ratios, but the light noble gases (He and Ne), like Genesis, are distinct from air.

Table 1
Compositional and Stable Isotope Systematics of Hoover-Diana and Genesis Separator Gases

	Compositions							Stable isotopes			
Sample	CH_4 (±2%)	C_2H_6 (±2%)	C_3 (±2%)	IC_4 (±2%)	NC_4 (±2%)	CO_2 (±2%)	N_2 (±2%)	$\delta^{13}C$ (CH_4) (±0.1‰)	$\delta^{13}C$ (C_2H_6) (±0.1‰)	$\delta^{13}C$ (CO_2) (±0.1‰)	δD (CH_4) (±1.0‰)
Hoover-Diana											
Hoover											
HA-2	91.66	3.63	2.51	0.471	0.39	0.06	0.87	−60.01	−31.48	n.d.	−214.5
HA-1	90.54	4.78	3.09	0.521	0.48	0.096	2.41	−57.80	−30.68	n.d.	−217.5
HA-5	89.18	4.11	2.65	0.407	0.356	0.12	0.25	−58.86	−31.66	n.d.	−212.6
Madison											
MP-1	88.86	4.77	3.83	0.856	0.8	0.12	0.24	−58.55	−30.72	n.d.	−212.1
South Diana											
SD-1	91.91	3.82	2.04	0.494	0.621	0.060	0.34	−56.64	−28.76	n.d.	−203.2
Genesis											
Pliocene											
A-7	89.41	4.32	3.13	0.568	1.16	0.27	0.15	−63.77	−32.57	−22.52	−203.3
A-7 (Dup)	89.31	4.31	3.18	0.582	1.19	0.27	0.15	−63.77	−32.71	−22.44	−201.7
A-12	84.41	5.90	4.41	0.863	1.87	0.23	0.16	−63.17	−33.32	−19.90	−204.9
A-16	87.74	4.36	3.16	0.642	1.48	0.35	0.16	−62.62	−32.65	−20.64	−203.7
Pleistocene											
A-15	84.37	7.52	4.33	0.750	1.39	0.26	0.26	−54.65	−31.59	−17.04	−209.1
A-3	87.59	4.72	3.18	0.621	1.39	0.41	0.20	−59.41	−32.45	−9.310	−202.4
A-5	88.26	5.41	3.28	0.585	1.09	0.28	0.23	−58.45	−31.84	−12.39	−202.9
A-2	85.26	6.14	3.85	0.725	1.49	0.33	0.23	−57.04	−31.89	−10.85	−207.2
A-1	87.00	5.94	3.61	0.640	1.20	0.38	0.23	−57.39	−32.05	−13.00	−204.2

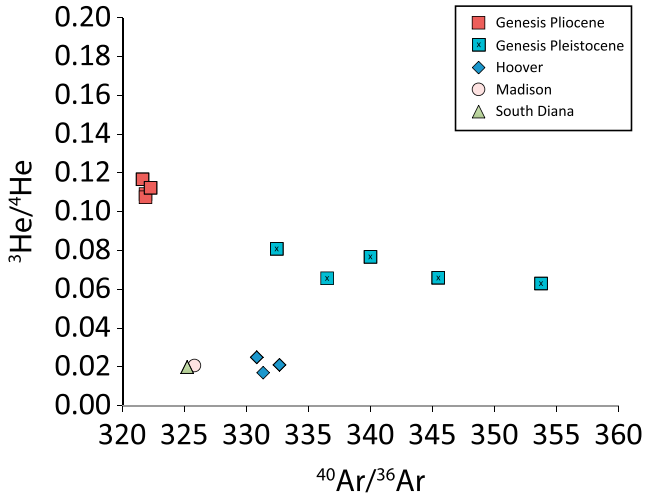

Figure 2. Helium isotopes ($^3He/^4He$) versus argon isotopes ($^{40}Ar/^{36}Ar$). Helium isotopes suggest that all Gulf of Mexico oils are dominantly radiogenic, with small mantle contributions. Hoover-Diana samples are the most radiogenic, with values approaching the production ratio of ^4He, whereas Pleistocene Genesis samples are intermediate and Pliocene Genesis samples contain the highest mantle ^3He contribution. Errors associated with measurements are encompassed by the size of the symbols.

Genesis helium (^4He) concentrations range from 0.3 to 10.2 × 10^{-6} cm^3STP/cm^3; samples are strongly radiogenic and have helium isotope ($^3He/^4He$) values ranging between 0.062 ± 0.002 and 0.117 ± 0.003 R_A, reported relative to the air value $R_A = 1.384 \times 10^{-6}$ (air = 1R_A; Clarke et al., 1976; Sano et al., 1988). Hoover-Diana helium (^4He) concentrations range from 2.9 to 17.5 × 10^{-6} cm^3STP/cm^3; samples are strongly radiogenic and have helium isotope ($^3He/^4He$) values ranging between 0.017 ± 0.001 and 0.025 ± 0.001 R_A (Figure 2). All noble gas data are reported in Table 2 along with 1σ uncertainties. Variations in $^3He/^4He$ ratios correspond to minor, yet resolvable, mantle He contributions. Using a two-component mixing model between subcontinental lithospheric mantle-like (6.1 R_A) and crustal (0.007 R_A) end-members (e.g., Ballentine & Burnard, 2002; Day et al., 2015), the percentage of crustal radiogenic ^4He varies between 98.2 and 99.0% in Genesis and between 99.7 and 99.8% in Hoover-Diana; therefore, we neglect discussion of mantle-derived noble gas sources.

Genesis neon (^{20}Ne) concentrations range from 4.0 to 6.5 × 10^{-9} cm^3STP/cm^3. Measured $^{20}Ne/^{22}Ne$ ratios vary between 9.94 ± 0.005 and 10.02 ± 0.005; these minor deviations from the atmospheric $^{20}Ne/^{22}Ne$ value of 9.8 are likely due to mass fractionation effects and/or a small mantle contribution. Measured $^{21}Ne/^{22}Ne$ ratios vary between 0.0305 ± 0.0001 and 0.0313 ± 0.0001. $^{21}Ne/^{22}Ne$ isotopic ratios in excess of the air value (0.0290) can be attributed to addition of nucleogenic-produced ^{21}Ne. Hoover-Diana neon (^{20}Ne) concentrations range from 2.3 to 14.6 × 10^{-9} cm^3STP/cm^3. Measured $^{20}Ne/^{22}Ne$ ratios vary between 9.74 ± 0.005 and 9.91 ± 0.005. Measured $^{21}Ne/^{22}Ne$ ratios vary between 0.0303 ± 0.0001 and 0.0309 ± 0.0001. $^{21}Ne/^{22}Ne$ isotopic ratios in excess of the air value (0.0290) can be attributed to nucleogenic crustal ^{21}Ne

Geochemistry, Geophysics, Geosystems

10.1029/2018GC007654

Table 2
Noble Gas (Helium, Neon, Argon, Krypton, and Xenon) Isotope Systematics of Hoover-Diana and Genesis Separator Gases

Sample	$^{4}He \times 10^{-6}$ cm^3 STP/cm^3	$^{20}Ne \times 10^{-9}$ cm^3 STP/cm^3	$^{40}Ar \times 10^{-6}$ cm^3 STP/cm^3	$^{84}Kr \times 10^{-12}$ cm^3 STP/cm^3	$^{132}Xe \times 10^{-12}$ cm^3 STP/cm^3	$^{3}He/^{4}He$ (R/R_A)	$^{20}Ne/^{22}Ne$	$^{21}Ne/^{22}Ne$	$^{40}Ar/^{36}Ar$	$^{86}Kr/^{84}Kr$	$^{132X}Xe/^{130}Xe$
Hoover-Diana											
Hoover											
HA-2	8.4 ± 0.1	6.96 ± 0.03	23.2 ± 0.12	4172 ± 4.2	583 ± 2.9	0.025 ± 0.001	9.82 ± 0.005	0.0308 ± 0.0001	330.8 ± 1.7	0.304 ± 0.001	6.60 ± 0.017
HA-1	10.1 ± 0.2	7.76 ± 0.04	24.0 ± 0.12	3992 ± 4.0	566 ± 2.8	0.017 ± 0.001	9.74 ± 0.005	0.0309 ± 0.0001	331.3 ± 1.7	0.304 ± 0.001	6.59 ± 0.017
HA-5	17.5 ± 0.3	13.8 ± 0.1	48.3 ± 0.24	8342 ± 8.3	1160 ± 6	0.021 ± 0.001	9.82 ± 0.005	0.0307 ± 0.0001	332.7 ± 1.7	0.304 ± 0.001	6.58 ± 0.017
Madison											
MP-1	10.0 ± 0.2	14.6 ± 0.1	27.8 ± 0.14	4505 ± 4.5	648 ± 3.2	0.019 ± 0.001	9.81 ± 0.005	0.0303 ± 0.0001	325.8 ± 1.6	0.303 ± 0.001	6.62 ± 0.017
South Diana											
SD-1	2.9 ± 0.1	2.35 ± 0.01	9.4 ± 0.05	2924 ± 2.9	953 ± 4.8	0.020 ± 0.001	9.91 ± 0.005	0.0307 ± 0.0001	325.2 ± 1.6	0.305 ± 0.001	6.62 ± 0.017
Genesis											
Pliocene											
A-7	6.0 ± 0.1	4.76 ± 0.02	20.6 ± 0.10	4814 ± 4.8	897 ± 4.5	0.107 ± 0.005	9.99 ± 0.005	0.0310 ± 0.0001	321.9 ± 1.6	0.307 ± 0.001	6.64 ± 0.017
A-7 (Dup)	6.0 ± 0.1	4.90 ± 0.02	20.4 ± 0.10	4818 ± 4.8	906 ± 4.5	0.117 ± 0.006	10.0 ± 0.005	0.0310 ± 0.0001	321.6 ± 1.6	0.306 ± 0.001	6.65 ± 0.017
A-12	2.9 ± 0.1	3.98 ± 0.02	22.3 ± 0.11	5701 ± 5.7	1171 ± 5.9	0.112 ± 0.006	10.0 ± 0.005	0.0310 ± 0.0001	322.3 ± 1.6	0.307 ± 0.001	6.65 ± 0.017
A-16	n.d.	4.87 ± 0.02	21.0 ± 0.10	4867 ± 4.9	927 ± 4.6	n.d.	9.94 ± 0.005	0.0305 ± 0.0001	324.7 ± 1.6	0.307 ± 0.001	6.65 ± 0.017
Pleistocene											
A-15	10.2 ± 0.2	6.31 ± 0.03	30.3 ± 0.15	5548 ± 5.5	905 ± 4.5	0.063 ± 0.003	9.96 ± 0.005	0.0310 ± 0.0001	353.7 ± 1.8	0.306 ± 0.001	6.65 ± 0.017
A-3	9.0 ± 0.1	6.06 ± 0.03	25.2 ± 0.13	5006 ± 5.0	824 ± 4.1	0.081 ± 0.004	10.00 ± 0.005	0.0310 ± 0.0001	332.4 ± 1.7	0.305 ± 0.001	6.62 ± 0.017
A-5	0.3 ± 0.1	6.41 ± 0.03	26.9 ± 0.13	5062 ± 5.1	832 ± 4.2	0.077 ± 0.004	10.02 ± 0.005	0.0312 ± 0.0001	340.0 ± 1.7	0.305 ± 0.001	6.63 ± 0.017
A-2	4.9 ± 0.1	6.03 ± 0.03	26.3 ± 0.13	5066 ± 5.1	791 ± 4.0	0.066 ± 0.003	9.99 ± 0.005	0.0313 ± 0.0001	336.5 ± 1.7	0.305 ± 0.001	6.63 ± 0.017
A-1	7.9 ± 0.1	6.45 ± 0.03	27.5 ± 0.14	5305 ± 5.3	921 ± 4.6	0.066 ± 0.003	9.97 ± 0.005	0.0309 ± 0.0001	345.4 ± 1.7	0.306 ± 0.001	6.65 ± 0.017

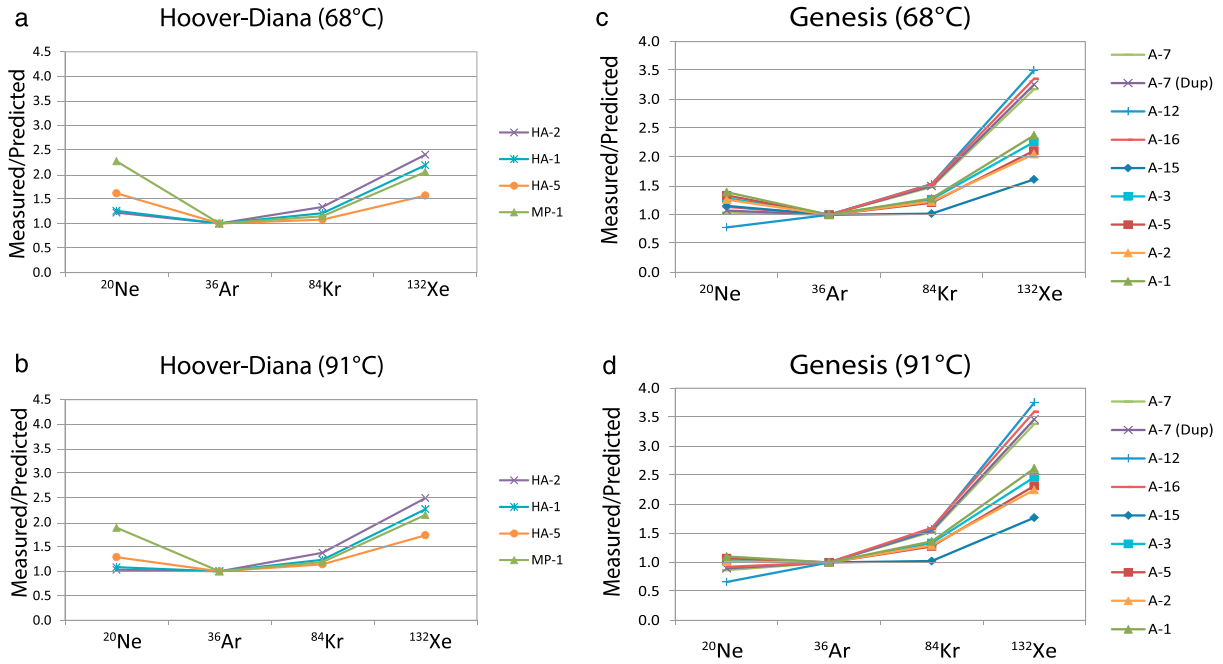

Figure 3. Measured versus predicted noble gas concentrations in oils (calculated using equation (2)) shown at both reservoir (68 °C) and migration (91 °C) temperatures. The model is set to unity for ^{36}Ar (i.e., observed = model predicted for each sample), showing agreement in the model between various noble gas species (i.e., ^{20}Ne, ^{84}Kr, and ^{132}Xe) of each sample. If unity is reached for each species, this would imply a coherent $\frac{V_o}{V_w}$ for the entire sample. At reservoir (68 °C) conditions (Figures 4a and 4c) there is a marked ^{20}Ne enrichment and heavy noble gas enrichment in measured samples (i.e., the model does not converge on one coherent $\frac{V_o}{V_w}$ for each sample). However, when migration temperatures (91 °C) are used (Figures 4b and 4d) to calculate exchange, there is significantly better agreement, particularly between ^{20}Ne and ^{36}Ar, suggesting that exchange likely occurred during migration.

addition. Deviations from the atmospheric ^{20}Ne/^{22}Ne value of 9.8 are likely due to mass fractionation effects or nucleogenic contributions.

Genesis argon (^{40}Ar) concentrations range from 20.4 to 30.3 × 10^{-6} cm^{3}STP/cm^3 and reveal significant deviations from the atmospheric ^{40}Ar/^{36}Ar value of 298.56 (Lee et al., 2006), with measured ^{40}Ar/^{36}Ar values varying between 322 ± 1.61 and 354 ± 1.77. These data show a resolvable contribution from a ^{40}Ar-rich source. In the absence of significant mantle-derived helium, it is assumed that this signal is from crustal radiogenic sources within the petroleum system. Measured ^{38}Ar/^{36}Ar values are predominantly air-like (0.1885; Lee et al., 2006; Burnard, 2013) and vary between 0.185 ± 0.003 and 0.189 ± 0.003. Hoover-Diana argon (^{40}Ar) concentrations range from 9.4 to 48.3 × 10^{-6} cm^{3}STP/cm^3 and also show similar deviations from the atmospheric ^{40}Ar/^{36}Ar value of 298.56 (Lee et al., 2006), with measured ^{40}Ar/^{36}Ar values varying between 325 ± 1.63 and 333 ± 1.66, suggesting a resolvable radiogenic ^{40}Ar contribution within the petroleum system. Argon isotopes (^{40}Ar/^{36}Ar) do not correlate to ^{20}Ne concentrations (Figure 3) and instead are relatively constant irrespective of ^{20}Ne. Measured ^{38}Ar/^{36}Ar values are predominantly air-like (0.1885; Lee et al., 2006; Burnard, 2013) and vary between 0.188 ± 0.003 and 0.189 ± 0.003.

Genesis krypton (^{84}Kr) concentrations range from 4.81 to 5.70 × 10^{-9} cm^{3}STP/cm^3 and from 2.92 to 8.34 × 10^{-9} cm^{3}STP/cm^3 in Hoover-Diana samples. Genesis samples are distinct from air (0.303; Aregbe et al., 1996) with respect to ^{86}Kr/^{84}Kr, ranging between 0.305 ± 0.003 and 0.307 ± 0.003, whereas Hoover-Diana samples range from 0.303 ± 0.003 to 0.305 ± 0.003, plotting just above the air-value (Table 2), which is likely due to mass dependent fractionation.

Genesis xenon (^{132}Xe) concentrations range from 791 to 1,171 × 10^{-12} cm^{3}STP/cm^3. Genesis ^{132}Xe/^{130}Xe values are air-like (6.60705; Pepin, 2000), ranging between 6.6245 ± 0.0165 and 6.6655 ± 0.0165 (Table 2) and are distinctly higher than air values. Hoover-Diana xenon (^{132}Xe) concentrations range from 556 to 1,160 × 10^{-12} cm^{3}STP/cm^3. Hoover-Diana ^{132}Xe/^{130}Xe values are air-like, ranging between 6.5809 ± 0.0165 and 6.6172 ± 0.0165, and are indistinguishable from air-values (Table 2).

Table 3
Oil Metadata, Solubility Coefficient, and Reconstructed Noble Gas Contents in Oil at RTP From Hoover-Diana and Genesis Separator Gases

Sample	API	Specific gravity g/cm^3	GOR	^{20}Ne mol/kg oil	^{36}Ar mol/kg oil	^{84}Kr mol/kg oil	^{132}Xe mol/kg oil	K_{WO} Ne atm kg/mol	K_{WO} Ar atm kg/mol	K_{WO} Kr atm kg/mol	K_{WO} Xe atm kg/mol
Hoover-Diana											
Hoover											
HA-2	24.7	0.906	130	2.9E−08	2.9E−07	1.7E−08	2.4E−09	577.1	565.4	123.8	60.7
HA-1	27.6	0.890	84[a]	3.3E−08	3.0E−07	1.7E−08	2.4E−09	543.9	520.0	126.4	56.2
HA-5	26.9	0.893	167	5.8E−08	6.1E−07	3.5E−08	4.8E−09	551.7	530.6	125.8	57.3
Madison											
MP-1	25.4	0.902	120	6.0E−08	3.5E−07	1.9E−08	2.7E−09	568.5	553.7	124.5	59.6
Genesis											
Pliocene											
A-7	28.8	0.883	268	3.6E−08	4.8E−07	3.6E−08	6.7E−09	529.5	500.3	127.5	54.3
A-7 (Dup)	28.8	0.883	268	3.7E−08	4.7E−07	3.6E−08	6.8E−09	529.5	500.3	127.5	54.3
A-12	30.8	0.872	148[a]	3.0E−08	5.2E−07	4.3E−08	8.9E−09	506.3	468.5	129.3	51.2
A-16	26.3	0.897	206	3.6E−08	4.8E−07	3.6E−08	6.8E−09	558.5	540.0	125.2	58.2
Pleistocene											
A-15	34.0	0.855	203	5.8E−08	6.6E−07	4.3E−08	7.0E−09	469.1	417.6	132.1	46.2
A-3	27.1	0.892	243	4.5E−08	5.6E−07	3.7E−08	6.1E−09	549.2	527.3	126.0	57.0
A-5	27.2	0.892	238	4.7E−08	5.9E−07	3.8E−08	6.2E−09	548.1	525.7	126.0	56.8
A-2	27.2	0.892	412	4.5E−08	5.8E−07	3.8E−08	5.9E−09	548.1	525.7	126.0	56.8
A-1	25.9	0.899	196	4.7E−08	5.9E−07	3.9E−08	6.8E−09	563.1	546.4	124.9	58.8

[a]Minimum values are used in calculations for each field. Note that all K_{WO} values are calculated at migration temperature (91 °C). All Hoover-Diana values are calculated at a salinity of 3.026 M, and all Genesis values are calculated at a salinity of 3.560 M.

5. Discussion

5.1. Reconstructing Noble Gas Concentrations in Oil

During the production process, an oil phase is transported from the reservoir to the surface, which results in decompression and gas exsolution from the oil phase. At the wellhead, the gas-to-oil ratio (GOR) is measured by combining the volume of gas to the volume of oil being produced at any given time. This GOR (units are m^3 of gas/m^3 of oil) can be combined with the specific gravity (SG) of the oil (units are g/cm^3) and the measured concentration (units are cm^{3}STP/cm^3) of a given noble gas in order to estimate the amount of noble gas that was originally in the oil phase (in units of mol/kg oil) prior to production and exsolution (see equation (1); e.g., Ballentine et al., 1996). This calculation assumes one mole of gas occupies 22.404 L at Standard Temperature and Pressure (STP).

$$\left[C_i^{oil}\right] = \frac{\left[C_i^{gas}\right](GOR)}{(SG)(22.404)} \quad (1)$$

In Table 2 we provide gas concentrations for all air-derived noble gas species $\left[C_i^{gas}\right]$ measured (units are cm^{3}STP/cm^3). In Table 3 we provide measured API gravity, GOR, and calculated concentrations in oil $\left[C_i^{oil}\right]$ (units are mol/kg oil). Density conversions (i.e., API to SG) and metric to imperial GOR conversions are detailed in Barry et al. (2018).

Importantly, we used *virgin GOR* estimates (i.e., lowest measured; 84 = Hoover-Diana; 148 = Genesis) when calculating noble gas contents in oil at reservoir conditions. Determining an accurate GOR is critical for converting measured gas concentrations into concentrations in the reservoir. However, the GOR that is measured at the wellhead is not always most representative of virgin GOR conditions, as this value will likely change significantly after a substantial period of production. Therefore, we opted to use the lowest (virgin) value for these calculations. The fact that there is very little variability in noble gas concentrations strongly suggests that at a constant GOR is most appropriate. For example, measured GORs vary by nearly a factor of 3 in the Genesis field, whereas measured noble gas concentrations in separator gases vary by less than 10% within a given reservoir interval (i.e., Pliocene versus Pleistocene).

5.2. Air-Derived Noble Gases

In order to assess the extent of interaction that an oil phase has had with ASW, the original noble gas inventory of ASW in the subsurface is first constrained. As with previous solubility models (e.g., Ballentine et al.,

Table 4
Calculated Oil/Water Volumetric Ratios in the Reservoir at Different Temperature and Salinity Conditions

Sample	^{20}Ne O/W[a]	^{36}Ar O/W[a]	^{84}Kr O/W[a]	^{132}Xe O/W[a]	^{20}Ne O/W[b]	^{36}Ar O/W[b]	^{84}Kr O/W[b]	^{132}Xe O/W[b]
Hoover-Diana								
Hoover								
HA-2	0.056	0.108	0.072	0.034	0.110	0.114	0.073	0.035
HA-1	0.046	0.099	0.077	0.036	0.089	0.104	0.078	0.036
HA-5	–	0.024	0.019	0.009	–	0.028	0.021	0.009
Madison								
MP-1	–	0.079	0.064	0.029	–	0.084	0.065	0.029
Genesis								
Pliocene								
A-7	0.071	0.053	0.024	0.005	0.085	0.054	0.025	0.005
A-7 (Dup)	0.066	0.054	0.024	0.005	0.080	0.055	0.025	0.005
A-12	0.114	0.044	0.017	0.001	0.125	0.045	0.018	0.001
A-16	0.060	0.054	0.023	0.004	0.077	0.056	0.024	0.004
Pleistocene								
A-15	0.012	0.023	0.018	0.006	0.026	0.025	0.020	0.006
A-3	0.006	0.037	0.021	0.006	0.041	0.041	0.022	0.006
A-5	–	0.034	0.021	0.006	0.033	0.037	0.022	0.006
A-2	0.008	0.035	0.021	0.007	0.042	0.038	0.022	0.007
A-1	–	0.034	0.018	0.004	0.030	0.038	0.019	0.004

Note. All Hoover-Diana values are calculated at a salinity of 3.026 M, and all Genesis values are calculated at a salinity of 3.560 M.
[a]Calculated at RTP (Hoover and Madison = 68 °C; Genesis Pliocene = 79 °C; Genesis Pleistocene = 68 °C). [b]Calculated at *migration temperatures*, which are the average temperature between generation and reservoir conditions (91 °C).

1996; Barry et al., 2016, 2017, 2018; Gilfillan et al., 2008; Zhou et al., 2005), it is assumed that air-derived noble gases (^{20}Ne, ^{36}Ar, ^{84}Kr, and ^{132}Xe) are originally input into the subsurface dissolved in water during aquifer recharge and/or during burial of air saturated pore fluids and subsequently isolated from further atmospheric inputs. Additionally, we assume that air-derived light noble gases (i.e., ^{20}Ne and ^{36}Ar) do not have any significant subsurface source, unlike radiogenic and/or mantle-derived noble gas isotopes. The solubility of noble gases in water is a function of recharge conditions (i.e., temperature, salinity, and recharge elevation); however, they increases with mass (Ne < Ar < Kr < Xe). The initial concentrations of ASW noble gas in formation waters can be approximated using empirically derived solubility coefficients (K_{GW}) at any given temperature and salinity (Crovetto et al., 1982; Smith, 1985; Smith & Kennedy, 1983).

5.3. Equilibrium Model

As an oil phase is generated and migrates from the source rock into the reservoir where it is stored, the noble gases are partitioned (K_{WO}) from ASW into the oil phase in a predictable way, which can be approximated using solubility coefficients (Kharaka & Specht, 1988). The resulting concentrations are determined by a number of parameters, including (1) the initial noble gas inventory in ASW ($\left[C_i^{asw}\right]$), (2) temperature and salinity conditions where phase exchange occurred (assumed to be the present-day reservoir conditions), and (3) the SG of the oil. Standard recharge conditions (i.e., seawater at 10 °C) are assumed for the first set of parameters. Reservoir temperature, salinity, and oil density (i.e., API or SG) are constrained for each sample as the wells are drilled and developed.

Using the estimates of initial noble gas concentrations in nondegassed oil ($\left[C_i^{oil}\right]$) in the reservoir (Table 3), solubility calculations (after Ballentine et al., 1996) are used to predict the relative volume of water that was in contact with an oil phase (assuming equilibrium conditions):

$$\frac{V_o}{V_w} = \frac{\left[C_i^{asw}\right]}{\left[C_i^{oil}\right]} - \left[\frac{K_{GO}^{M}}{(SG)\left(K_{GW}^{M}\right)}\right] \quad (2)$$

The solubility coefficients between gas and water (K_{GW}^{M}) are controlled by reservoir temperature and salinity (Crovetto et al., 1982; Smith, 1985; Smith & Kennedy, 1983). The solubility coefficients between gas and oil (K_{GO}^{M}) are controlled by reservoir temperature, salinity, and the SG of the oil (Kharaka & Specht,

1988). In this way we calculate the volume ratio of oil to water, $\frac{V_o}{V_w}$ (Table 4), at reservoir and average migration pathway conditions using equation (2).

5.4. Model Sensitivity: Implications for Exchange and Migration

In the GOM systems, reservoir temperature range between 55 and 82 °C; however, generation temperatures of hydrocarbons in the source interval were much higher. Indeed, methane clumped isotopes record temperatures of up to 118 °C for the Hoover field (Douglas et al., 2017), and up to 110 °C for the Genesis field (Stolper et al., 2018), consistent with estimates of fluid maturity based on biomarker ratios of oil compounds. The temperatures of carrier beds along which hydrocarbons migrated from the source rock to the present-day traps therefore occupy the range between generation and present-day reservoir temperatures. This range in temperatures provides a wide range of conditions under which noble gases can exchange, and thus, we calculate a *migration temperature* of 91 °C, which is simply an average between generation and reservoir temperature conditions. Predicted values from the model are then compared with reconstructed noble gas concentrations in oil, which are determined by considering the virgin GOR of the system (i.e., minimum value measured in each field, respectively).

Notably, the model is extremely sensitive to temperature, salinity, and GOR, which control solubility exchange. For example, we calculate a $\frac{V_o}{V_w}$ (^{20}Ne) of 0.056 for sample HA-2 at reservoir temperature (68 °C) and pressure (RTP), and a $\frac{V_o}{V_w}$ 0.110 if a migration temperature of 91 °C is used for the point of exchange. This illustrates the sensitivity of the neon model to exchange temperatures (i.e., a 23 °C increase in the exchange temperature results in a twofold increase in predicted $\frac{V_o}{V_w}$). However, for other species (i.e., Ar, Kr, and Xe), the increase in exchange temperature has a much less pronounced effect on the modeling results under simple exchange conditions. The model returns tangible (i.e., non-negative) results 94% of the time; however, for some Hoover and Madison samples (i.e., HA-5, MP-1), it is impossible to acquire observed ^{20}Ne concentrations at RTP or migration temperature using the equilibrium solubility model applied here. For example, sample MP-1 has both a high [^{20}Ne] concentration in oil and a higher ^{20}Ne/^{36}Ar value than can be produced in any solubility scenario, suggesting an additional processes such as extraneous air addition, potentially associated with well-development, hydraulic fracturing, and/or secondary stimulation of the well. Notably, an air-like noble gas signal was recently reported in oil wells that have been subjected to extensive enhanced oil recovery (Barry et al., 2018) suggesting that the excess air signature is introduced during well-development and/or production. The model returns acceptable results for Ar, Kr, and Xe 100% of the time, but only about 80% of the time for Ne. This observation puts important bounds on model assumptions, as a solution is required that can explain as much of the data as possible, considering that exchange conditions were likely similar for all samples in each reservoir.

In Figures 3a–3d we show the measured noble gas concentration in oils versus reconstructed values (equation (2)) at different temperatures (i.e., RTP, 68 °C, or migration, 91 °C). We used an inverse approach, whereby the model is set to unity for ^{36}Ar (i.e., observed = model for each sample) and thus a different $\frac{V_o}{V_w}$ is predicted for each species (^{20}Ne, ^{84}Kr, and ^{132}Xe) of each sample. At RTP conditions (Figures 3a and 3c) there is a marked ^{20}Ne enrichment and heavy noble gas enrichment in measured samples (i.e., the model does not converge on one coherent $\frac{V_o}{V_w}$ for each sample). However, when migration temperatures (91 °C) are used to calculate exchange, there is significantly better agreement, particularly between ^{20}Ne and ^{36}Ar. When taken together, these results indicate that exchange most likely occurred at migration temperatures (i.e., intermediate between generation and reservoir conditions). It is not surprising that we observe a divergence in modeling results for heavy noble gases as there is systematic heavy noble gas (Kr-Xe) enrichment relative to the light noble gases, which is a phenomenon that has been previously observed in other hydrocarbon systems (e.g., Byrne et al., 2017; Torgersen & Kennedy, 1999) and is discussed in detail in section 5.4.

In this section, we present the details of an equilibrium model, which assumes that the oil phase is in direct contact with the water and that equilibrium has been reached at either reservoir (based on inverse modeling and wellhead data) or migration conditions (based on averaging clumped isotope generation temperatures, reservoir temperatures, and reservoir salinities). The first scenario assumes that oil has been generated and expelled from the source rock and migrated to the reservoir, where the bulk of noble gas exchange occurs at RTP. The second scenario represents a situation where oil is also generated and expelled from the

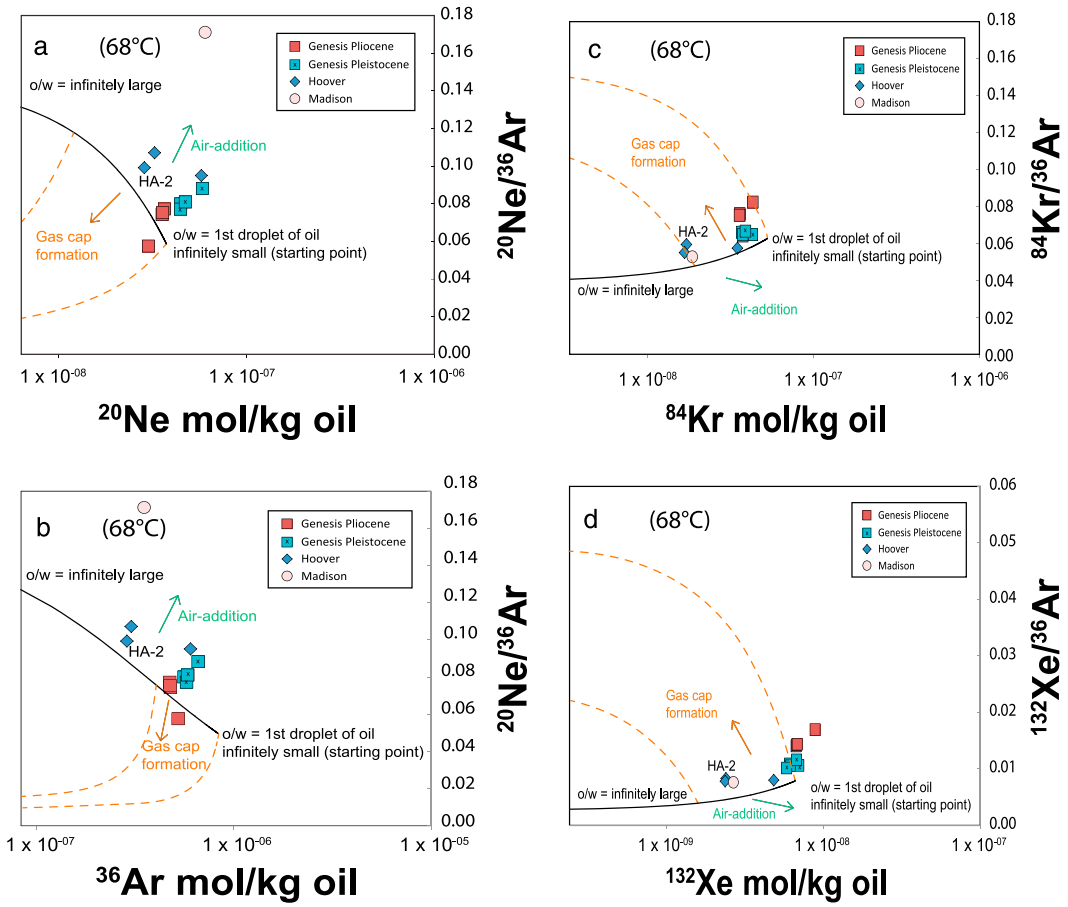

Figure 4. Reconstructed noble gas concentrations in oil (calculated using equation (1)) versus measured elemental ratios. All partitioning is calculated at reservoir temperate. Errors associated with measurements are encompassed by the size of the symbols. Overlain is the predicted geochemical evolution based on the solubility model described in section 5.3 (equation (2)). The predicted trajectory of oil—as it interacts with water—is shown as a solid black line; this line evolves from right to left, with a *starting point* marked by an infinitely small $\frac{V_o}{V_w}$ and evolving toward an infinitely large $\frac{V_o}{V_w}$. The secondary effect of gas cap formation on oil is shown as dashed orange lines. The envelope—formed by the solid black and dashed orange lines—represents the predicted residual oil signature following gas cap formation. Any values that fall outside of this envelope require air-addition (i.e., green arrow), which can be attributed to well-development practices, fracking, and/or surface contamination during sampling.

source rock, but it acquires most of its noble gas inventory during transport to the reservoir (at higher migration temperatures). We suggest that in the case of longer distance transfer from depth to shallow reservoirs, interaction with groundwater predominantly occurs during the migration route, rather than within the reservoir. This is because the migration pathway from the source rock to a trapping structure is likely to be a relatively porous and permeable lithology that is water-saturated, and often hosts formation water extends regionally. In addition, most accepted migration models suggest transport through a water-phase. As such, migration of a hydrocarbon phase through this rock-unit will inevitably result in some hydrocarbon-water exchange. Migration pathways can vary in their length-scale from short, in the case of some unconventional systems with interbedded sandstones and source intervals (e.g., Bakken shale), to long, that is (many hundreds of kilometers; Lawson et al., 2018). These findings have profound implications for how and where fluids interact in hydrocarbon systems, and thus the volumetric ratios that are predicted using equilibrium solubility models.

In Figures 4 and 5 we show the predicted evolution of the oil phase at different $\frac{V_o}{V_w}$. The predicted trends are shown at both reservoir conditions (68 °C; Figures 4a–4d) and migration temperatures (91 °C; Figures 5a–5d). Where the two predictive trends converge, the $\frac{V_o}{V_w}$ = *first droplet* (i.e., there is an infinitesimally small volume of oil *stripping* noble gases). This first droplet point represents the point where there is essentially only water in the system (just as the first droplet of oil is beginning to be generated) and thus an infinitely small $\frac{V_o}{V_w}$. As the

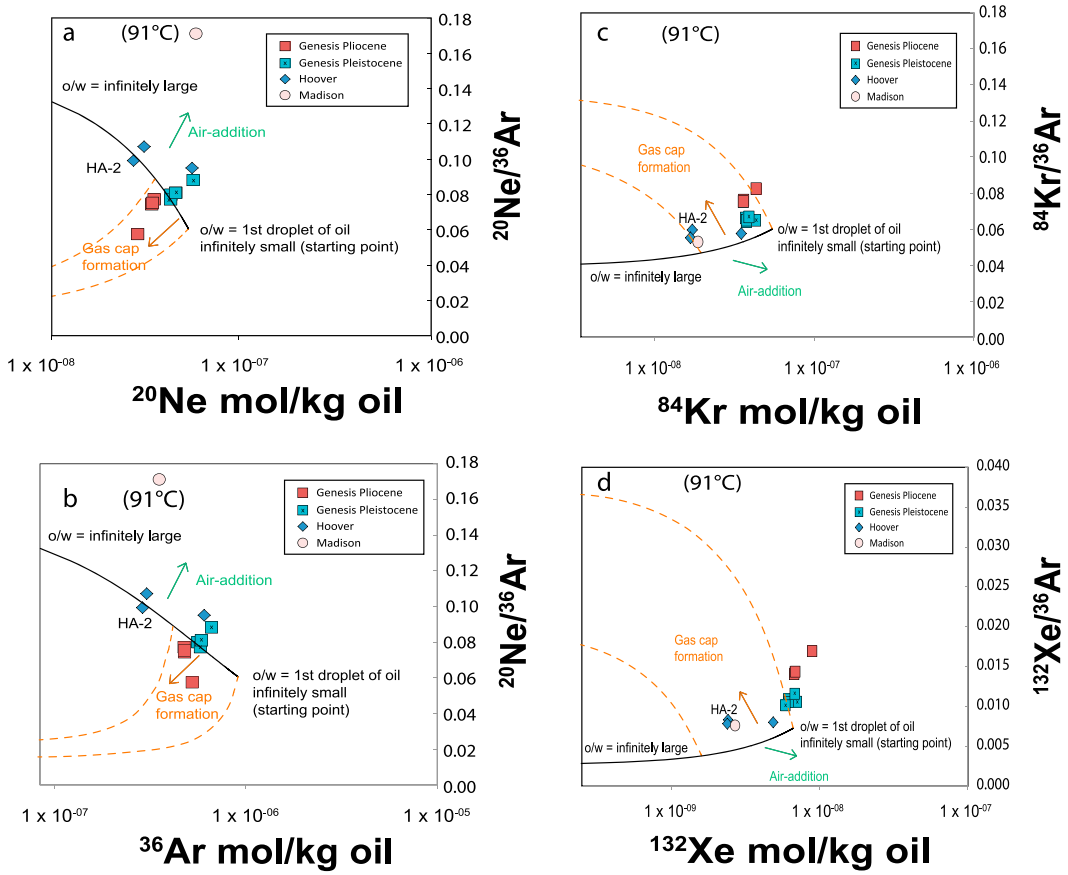

Figure 5. Reconstructed noble gas concentrations in oil (calculated using equation (1)) versus measured elemental ratios. All partitioning is calculated at migration temperate.

amount of oil relative to water increases, the predicted concentrations in noble gases in the oil phase evolves to the left in Figures 4a and 4b—toward lower concentrations in the oil (i.e., $\frac{V_o}{V_w}$ approach infinity). This is due to the fact that there is a limited initial inventory of noble gases (originally in the water phase) and thus, as oil migrates past a water column—that is assumed to be stagnant over the timescale of hydrocarbon migration through the column—noble gases are stripped out of the water due to solubility exchange with oil; this process acts to effectively dilute the concentration in the oil phase as $\frac{V_o}{V_w}$ increases. The predicted effects of gas cap formation on the oil phase (see section 5.3) are also shown in Figures 4 and 5 as orange dashed lines. Likewise, if a gas cap were to form, the system would also evolve to the left (as the noble gases partition from an oil phase into a gas phase), again, moving toward lower oil concentrations (i.e., $\frac{V_g}{V_o}$ approaching infinity).

Oils from the Hoover and Madison fields have predicted $\frac{V_o}{V_w}$ values (Table 4) that are 2–3 times greater than those of the Genesis reservoirs based on an average of the $\frac{V_o}{V_w}$ derived from the equilibrium solubility model for Ne and Ar. We do not include Kr and Xe results in the average calculations, given the potential for addition of lithology-derived heavy noble gases to those derived solely from the formation water (i.e., heavy noble gases are preferentially adsorbed onto source rocks such as shale). The higher calculated $\frac{V_o}{V_w}$ in Hoover-Diana versus Genesis (Table 4) can be interpreted in two different ways: either (1) the Hoover reservoir interval has 2–3 times more oil than any of the individual Genesis reservoirs, which is consistent with independent estimates of oil in place for the respective reservoirs, or (2) Genesis oils have experienced longer migration pathways than Hoover-Diana oils and thus have interacted with more water. The latter interpretation is consistent with the observation that Genesis oils are sourced from a deeper Jurassic interval in the Genesis minibasin, whereas Hoover-Diana samples are sourced from a shallower Tertiary source interval in the Hoover-Diana minibasin and therefore a shorter migration distance.

Importantly, the disparity between calculated Hoover-Diana and Genesis $\frac{V_o}{V_w}$ (Table 4) agrees with our current understanding of oil volumes in place in the two petroleum systems, respectively; in total, the Hoover-Diana field has a stock tank oil in place (STOIIP) of 140 million barrels versus 380 million barrels at Genesis (C&C Reservoirs, 2010, 2011). However, there is a significant difference between the two fields in that Hoover-Diana is a single reservoir interval, whereas Genesis is a stacked system with five oil bearing reservoirs. If we assume equal volumes in each reservoir, we estimate approximately 76 million barrels per reservoir at Genesis, which is approximately half as much oil per reservoir than at Hoover; this observation is consistent with the first interpretation of the $\frac{V_o}{V_w}$ in Table 4 (i.e., 2–3 times more oil in Hoover-Diana). We also note that the Genesis system likely has a much longer migration pathway, based on biomarker data and the law of superposition. In the Genesis minibasin, hydrocarbon fluids migrate from a deep Jurassic source rock to the reservoir interval, whereas hydrocarbon fluids migrate from a relatively shallower Tertiary source rock in the Hoover-Diana minibasin. This qualitatively would support more interaction with water during migration form source to reservoir in the Genesis fluids, and thus lower $\frac{V_o}{V_w}$, which would lend credence to the second interpretation. Importantly, the two interpretations of the disparity between modeled $\frac{V_o}{V_w}$ are not mutually exclusive.

In a broader context, the fact that the noble gas model produces $\frac{V_o}{V_w}$ results that are consistent with geologic observations (i.e., aquifer volume/oil ratios and known migration distances) for GOM samples, suggests that the model is well calibrated. The implication is that a variation of this three-phase noble gas model could be further developed into a viable exploration technique; if volumetric hydrocarbon ratios could be combined with independent estimates of hydrocarbon migration distance and/or formation fluid volumes (using known stratigraphy), then this geochemical technique could potentially be used to differentiate between large and small oil accumulations.

5.5. Model Sensitivity: Gas Cap Formation

The solubility model presented in section 5.1 assumes simple two-component exchange between ASW and an oil phase. However, if a gas cap formed in the reservoir—effectively making it a three-phase (oil-water-gas) system, the model will also predict the effect on the residual oil phase (Figures 3a and 3b). As a gas cap forms, noble gases are preferentially partitioned from the oil phase into the gas phase according to Henry's law (i.e., light noble gases, which are less soluble, will preferentially partition into the gas cap relative to heavier noble gases, and thus, estimates of the original oil composition ($[C_i^{oil}]$), calculated using equation (1), are overestimates of the original oil noble gas content and $\frac{V_o}{V_w}$ estimates are also overestimates. There are an infinite number of possible three-component exchange scenarios, so we select the gas cap trend that provides the best fit through each sample. The predicted gas cap trend is calculated according to equation (3):

$$\left[C_{gc}^{oil}\right] = \frac{\left[C_i^{oil}\right]}{\left(\frac{[22.4][SG]\left[\frac{V_o}{V_G}\right]}{273.15\left(K_{GO}^{M}\right)+1}\right)} \tag{3}$$

where the concentration in oil following gas cap formation is $\left[C_{gc}^{oil}\right]$. We iteratively run this model, varying $\frac{V_o}{V_G}$ in order to produce a single trend line. If the model is run at end-member conditions (i.e., $\frac{V_o}{V_G}$ = approaching 0; $\frac{V_o}{V_G}$ = approaching infinity) a *gas cap envelope* can be determined (e.g., Figures 4 and 5). If data fall in this envelope, it means that an equilibrium three-component mixture can explain the data. K_{GO}^{M} is the salinity, temperate, and SG modified solubility coefficient between gas and oil. Where any individual calculated trend intersects with the oil-water solubility trend, we are able to determine the original oil composition ($[C_i^{oil}]$) that is required to have lost a gas cap to form the observed values. An underlying assumption of such a model is that oil-water exchange occurred first, followed by subsequent gas cap formation. This is best illustrated when noble gas concentration data are combined with elemental ratio data (Figures 4 and 5). When the correction for gas cap formation is made, this changes the calculated $\frac{V_o}{V_w}$ to a smaller value compared with the assumption of no gas cap. Following the previous example of sample HA-2, we calculated a $\frac{V_o}{V_w}$ (^{20}Ne) of 0.110 at migration temperature (91 °C); however, when the effect of gas cap formation is considered,

this estimate will decrease by a negligible amount to a $\frac{V_o}{V_w}$ (^{20}Ne) of 0.109, suggesting that a voluminously significant gas cap did not form. This scenario can be visualized in Figure 5a, where the point of intersection between the black solid O-W solubility fractionation line and the orange dashed gas cap formation line would be used to determine the $\frac{V_o}{V_w}$ value (Figure 5a).

Notably, gas cap formation is plausible considering geological constraints. The Diana field in the Hoover-Diana minibasin is composed of two phases: a liquid oil leg below a large gas cap leg at the top. Genesis does not currently have a large gas cap. However, these modeling results strongly suggest that Genesis must have previously had a gas cap of a similar relative size to that of Diana. Independent evidence (i.e., the large adjacently located Popeye gas field) suggests that the Genesis could have previously formed and lost a gas cap. Interestingly, methane clumped isotope constraints suggest that the Genesis Pliocene oils may have charged the reservoir at a lower temperature than we see at present day. Under those PVT conditions it is conceivable to form a gas cap that subsequently leaked and migrated to charge overlying or updip structures.

5.6. Heavy Noble Gas Enrichments

There are clear heavy noble gas excesses in these GOM solution oils relative to what is predicted from simple solubility exchange with ASW (Figures 3a–3d). As a result, solubility models are unable to accurately predict volumetric $\frac{V_o}{V_w}$ (Table 4) using the heavy noble gases. Such heavy noble gas enrichments have previously been discussed in detail (Byrne et al., 2017; Torgersen & Kennedy, 1999; Zhou et al., 2005). In source-rock lithologies with extensive organic material, such as shales and cherts, and in marine sediment hosted reservoirs, Kr and Xe have been shown to preferentially absorb onto minerals (e.g., Pitre & Pinti, 2010; Podosek et al., 1981) relative to He, Ne, and Ar. If such heavy noble gas encumbered lithologies are buried to pressures and temperatures where hydrocarbons are generated, the hydrocarbons may inherit heavy noble gas enrichments (Hiyagon & Kennedy, 1992; Torgersen & Kennedy, 1999; Zhou et al., 2005). For example, it was noted that there was an approximately constant carbon to sedimentary-derived xenon ratio in the methane generated by the San Juan Basin (USA) coalbed methane system (Zhou et al., 2005). We surmise that the heavy noble gas signatures in GOM oils are likely modified by fluid-rock interaction, whereby sediments, which are enriched in sorbed (heavy) noble gases, transfer their heavy noble gas enrichment into the hydrocarbon phase during hydrocarbon expulsion. These processes could occur either sequentially or simultaneously. Figures 3a–3d illustrate that heavy noble (Kr and Xe) gases are enriched in gases derived from oils, thus yielding lower $\frac{V_o}{V_w}$ than estimates derived from Ne and Ar measurements. Due to known additions, these Kr-Xe data should be considered with caution.

5.7. Radiogenic Isotopes

Noble gases are useful for understanding formation and migration processes; however, they can also be used to determine valuable temporal information about subsurface fluid movement and storage mechanisms. Radiogenic noble gas isotopes (e.g., ^{4}He) are continually produced in Earth's crust by decay of parent isotopes (e.g., ^{238}U, ^{235}U, and ^{232}Th), and their signatures are subsequently imparted ubiquitously into connate and formation fluids. As these radiogenic-rich fluids interact with an oil phase—either during migration or in the reservoir—the radiogenic signatures are imparted into the oils, which are initially devoid of noble gases. Due to the fact that noble gases are variably soluble in oils, the concentration of radiogenic noble gases within hydrocarbon reservoirs is controlled by the extent of oil interaction with formation fluids in exactly the same way as air-derived noble gases (see section 5.1).

Helium isotopes show that all GOM oils are strongly radiogenic, with He-isotope values ranging from 0.017 to 0.117 R_A (Figure 1). Hoover-Diana samples are the most radiogenic, whereas Pleistocene Genesis samples are intermediate and Pliocene Genesis samples contain the highest mantle He contribution. This suggests that mantle contributions to the system are typically less than 2%, and this small amount of mantle contribution is accounted for in the age calculations below. These findings are consistent with other strongly radiogenic He isotopic ratios observed in a variety of hydrocarbon systems (e.g., Byrne et al., 2017).

Noble gas partitioning models suggest that GOM oils were isolated in closed systems and then subsequently modified by gas cap formation. Genesis is thought to have behaved as an open system, whereas the gas in Diana remained behind and thus acted as a closed system. By assuming (1) both groundwater-derived noble gases (e.g., ^{20}Ne and ^{36}Ar) and crustal radiogenic noble gases (e.g., ^{4}He) are coherently fractionated according

to known relative partitioning behavior (i.e., Ki/Kj), irrespective of their source; (2) *in situ reservoir* and *source rock-derived* radiogenic contributions are negligible relative to those acquired through hydrocarbon-groundwater exchange; and (3) GOM is originally a simple closed system and thus any open system gas cap formation processes can be accounted for, then the measured concentration of radiogenic ^{4}He in the gas phase of a given sample can be used to estimate the initial concentration of ^{4}He. This initial concentration represents the amount that is required to have originally been in the water that was subsequently stripped of its noble gases by interaction with oil, to eventually form the separator gases that we measure in wells.

Using the methods of Zhou and Ballentine (2006), we calculate an average residence-time for oil of 4 Ma for Hoover-Diana and Madison, whereas Genesis samples yielded an average residence time of 4.5 Ma. The extent of ingrowth and subsequent exchange is also a function of rock thickness and porosity. For Hoover-Diana, we assumed a thickness of 7 m and a porosity of 34% (Moyer et al., 2001). For Genesis, we assume a thickness of 15 and a porosity of 30% (Sweet & Sumpter, 2007). Notably, both thickness estimates are conservative, as some units are up to 45 m thick in Hoover and 30 m thick in Genesis. This calculation also assumes an external accumulation rate of 2.31×10^{-6} cm^{3}STP^{4}He/cm^2 (after Zhou & Ballentine, 2006). These ages are geologically reasonable as they are younger than depositional ages (~5 Ma), but older than hydrocarbon charge ages (~3 Ma).

6. Summary

We have presented the details of a noble gas solubility model that utilizes produced gas He-Ne-Ar-Kr-Xe data to quantify solubility exchange in a complex three-component hydrocarbon system. To our knowledge, this is the first study to use all of the stable noble gas isotopes to understand hydrocarbon charge, migration, and emplacement mechanisms in a complex three-component hydrocarbon system. This model can be used to predict relative volumes of oil versus water in the subsurface, which when considered in the context of independently determined estimates of hydrocarbon migration distance and/or formation water volumes has the potential to be used as a predictive measure for the size of an oil accumulation.

Noble gas isotope data from two oil-bearing minibasins in the GOM-Genesis and Hoover-Diana were used for initial calibration of our model. We find the following:

(1) Noble gas abundance data can be best explained by a three-phase (gas-water-oil) system, which we interpret to reflect gas cap formation in the reservoir following initial noble exchange between oil and water during hydrocarbon migration.
(2) Equilibrium solubility models based on ^{20}Ne and ^{36}Ar concentrations suggest that the Hoover and Madison fields have $\frac{V_o}{V_w}$ that are 2–3 times greater on average than Genesis reservoir fluids. This can be explained by a larger volume of oil in the Hoover and Madison fields relative to the Genesis reservoirs. Alternatively, the disparity in calculated $\frac{V_o}{V_w}$ may reflect the longer migration pathway from the Jurassic source at Genesis and the potential for greater interaction with formation water prior to charging the reservoirs.
(3) Helium accumulation ages of 4–4.5 Ma for the Hoover, Madison, and Genesis reservoir fluids are consistent with geologic constraints of likely oil-water interaction and are between the depositional age ($<$5 Ma) of the reservoir interval and models of hydrocarbon generation timing (~ 3 Ma).

With further development and refinement, the noble gases technique has the potential to be widely applied for the purpose of understanding fluid exchange processes in a complex hydrocarbon system.

Acknowledgments
We thank ExxonMobil for funding and providing the samples. In addition, we thank James Scott and two anonymous reviewers for their comprehensive and constructive reviews, as well as Janne Blichert-Toft for editorial handling.

References

Aeschbach-Hertig, W., & Solomon, D. K. (2013). Noble gas thermometry in groundwater hydrology. In *The noble gases as geochemical tracers*, (pp. 81–122). Berlin Heidelberg: Springer. https://doi.org/10.1007/978-3-642-28836-4_5

Aregbe, Y., Valkiers, S., Mayer, K., & De Bièvre, P. (1996). Comparative isotopic measurements on xenon and krypton. *International Journal of Mass Spectrometry Ion Processes*, *153*(1), L1–L5.

Ballentine, C. J., Burgess, R., & Marty, B. (2002). Tracing fluid origin, transport and interaction in the crust. *Reviews in Mineralogy and Geochemistry*, *47*, 539–614. https://doi.org/10.2138/rmg.2002.47.13

Ballentine, C. J., & Burnard, P. G. (2002). Production, release and transport of noble gases in the continental crust. *Reviews in Mineralogy and Geochemistry*, *47*(1), 481–538. https://doi.org/10.2138/rmg.2002.47.12

Ballentine, C. J., & Hall, C. M. (1999). Determining paleotemperature and other variables by using an error-weighted, nonlinear inversion of noble gas concentrations in water. *Geochimica et Cosmochimica Acta*, *63*(16), 2315–2336. https://doi.org/10.1016/S0016-7037(99)00131-3

Ballentine, C. J., O'Nions, R. K., & Coleman, M. L. (1996). A Magnus opus: Helium, neon, and argon isotopes in a North Sea oilfield. *Geochimica et Cosmochimica Acta*, *60*(5), 831–849. https://doi.org/10.1016/0016-7037(95)00439-4

Ballentine, C. J., O'nions, R. K., Oxburgh, E. R., Horvath, F., & Deak, J. (1991). Rare gas constraints on hydrocarbon accumulation, crustal degassing and groundwater flow in the Pannonian Basin. *Earth and Planetary Science Letters*, *105*(1-3), 229–246. https://doi.org/10.1016/0012-821X(91)90133-3

Barry, P. H., Hilton, D. R., Day, J. M., Pernet-Fisher, J. F., Howarth, G. H., Magna, T., et al. (2015). Helium isotopic evidence for modification of the cratonic lithosphere during the Permo-Triassic Siberian flood basalt event. *Lithos*, *216*, 73–80.

Barry, P. H., Kulongoski, J. T., Landon, M. K., Tyne, R. L., Gillespie, J. M., Stephens, M. J., et al. (2018). Tracing enhanced oil recovery signatures in casing gases from the Lost Hills oil field using noble gases. *Earth and Planetary Science Letters*, *496*(2018), 57–67. https://doi.org/10.1016/j.epsl.2018.05.028

Barry, P. H., Lawson, M., Meurer, W. P., Danabalan, D., Byrne, D. J., Mabry, J. C., & Ballentine, C. J. (2017). Determining fluid migration and isolation times in multiphase crustal domains using noble gases. *Geology*, *45*(9), 775–778. https://doi.org/10.1130/G38900.1

Barry, P. H., Lawson, M., Meurer, W. P., Warr, O., Mabry, J. C., Byrne, D. J., & Ballentine, C. J. (2016). Noble gases solubility models of hydrocarbon charge mechanism in the Sleipner Vest gas field. *Geochimica et Cosmochimica Acta*, *194*, 291–309. https://doi.org/10.1016/j.gca.2016.08.021

Bosch, A., & Mazor, E. (1988). Natural gas association with water and oil as depicted by atmospheric noble gases: Case studies from the southeastern Mediterranean Coastal Plain. *Earth and Planetary Science Letters*, *87*(3), 338–346. https://doi.org/10.1016/0012-821X(88)90021-0

Byrne, D. J., Barry, P. H., Lawson, M., & Ballentine, C. J. (2017). Noble gases in conventional and unconventional petroleum systems. *Geological Society, London, Special Publications*, *468*(1), 127–149.

Byrne, D. J., Barry, P. H., Lawson, M., & Ballentine, C. J. (2018). Determining gas expulsion vs retention during hydrocarbon generation in the Eagle Ford Shale using noble gases. *Geochimica et Cosmochimica Acta*, *241*, 240–254. https://doi.org/10.1016/j.gca.2018.08.042

Burnard, P. (2013). *The noble gases as geochemical tracers*. Springer.

C&C Reservoirs (2010). Genesis Field, Gulf of Mexico, USA. Field evaluation report, North America. Digital Analogs, 53 pp.

C&C Reservoirs (2011). Hoover & Diana Fields Alamos Canyon & East Breaks Area Gulf of Mexico, USA. Field Evaluation Report, North America. Digital Analogs, 60 pp.

Castro, M. C., Goblet, P., Ledoux, E., Violette, S., & de Marsily, G. (1998). Noble gases as natural tracers of water circulation in the Paris Basin. 2. Calibration of a groundwater flow model using noble gas isotope data. *Water Resources Research*, *34*, 2467–2483. https://doi.org/10.1029/98WR01957

Castro, M. C., Jambon, A., Marsily, G., & Schlosser, P. (1998). Noble gases as natural tracers of water circulation in the Paris Basin: 1. Measurements and discussion of their origin and mechanisms of vertical transport in the basin. *Water Resources Research*, *34*, 2443–2466. https://doi.org/10.1029/98WR01956

Clarke, W. B., Jenkins, W. J., & Top, Z. (1976). Determination of tritium by mass spectrometric measurement of 3 He. *The International Journal of Applied Radiation and Isotopes*, *27*(9), 515–522.

Cook, P. G., Solomon, D. K., Sanford, W. E., Busenberg, E., Plummer, L. N., & Poreda, R. J. (1996). Inferring shallow groundwater flow in saprolite and fractured rock using environmental tracers. *Water Resources Research*, *32*, 1501–1509. https://doi.org/10.1029/96WR00354

Crovetto, R., Fernández-Prini, R., & Japas, M. L. (1982). Solubilities of inert gases and methane in H2O and in D2O in the temperature range of 300 to 600 K. *The Journal of Chemical Physics*, *76*, 1077–1086. https://doi.org/10.1063/1.443074

Darrah, T. H., Jackson, R. B., Vengosh, A., Warner, N. R., Whyte, C. J., Walsh, T. B., et al. (2015). The evolution of Devonian hydrocarbon gases in shallow aquifers of the northern Appalachian Basin: Insights from integrating noble gas and hydrocarbon geochemistry. *Geochimica et Cosmochimica Acta*, *170*, 321–355.

Darrah, T. H., Vengosh, A., Jackson, R. B., Warner, N. R., & Poreda, R. J. (2014). Noble gases identify the mechanisms of fugitive gas contamination in drinking-water wells overlying the Marcellus and Barnett Shales. *Proceedings of the National Academy of Sciences*, *111*(39), 14076–14081.

Day, J. M., Barry, P. H., Hilton, D. R., Burgess, R., Pearson, D. G., & Taylor, L. A. (2015). The helium flux from the continents and ubiquity of low-3 He/4 He recycled crust and lithosphere. *Geochimica et Cosmochimica Acta*, *153*, 116–133.

Douglas, P. M., Stolper, D. A., Eiler, J. M., Sessions, A. L., Lawson, M., Shuai, Y., et al. (2017). Methane clumped isotopes: Progress and potential for a new isotopic tracer. *Organic Geochemistry*, *113*. https://doi.org/10.1016/j.orggeochem.2017.07.016

Galloway, W. E., Ganey-Curry, P. E., Li, X., & Buffler, R. T. (2000). Cenozoic depositional history of the Gulf of Mexico basin. *AAPG Bulletin*, *84*(11), 1743–1774.

Gilfillan, S. M., Ballentine, C. J., Holland, G., Blagburn, D., Lollar, B. S., Stevens, S., et al. (2008). The noble gas geochemistry of natural CO_2 gas reservoirs from the Colorado Plateau and Rocky Mountain provinces, USA. *Geochimica et Cosmochimica Acta*, *72*(4), 1174–1198.

Gilfillan, S. M., Lollar, B. S., Holland, G., Blagburn, D., Stevens, S., Schoell, M., et al. (2009). Solubility trapping in formation water as dominant CO_2 sink in natural gas fields. *Nature*, *458*(7238), 614–618.

Hiyagon, H., & Kennedy, B. M. (1992). Noble gases in CH4-rich gas fields, Alberta, Canada. *Geochimica et Cosmochimica Acta*, *56*(4), 1569–1589.

Holland, G., Lollar, B. S., Li, L., Lacrampe-Couloume, G., Slater, G. F., & Ballentine, C. J. (2013). Deep fracture fluids isolated in the crust since the Precambrian era. *Nature*, *497*, 357–360. https://doi.org/10.1038/nature12127

Hood, K. C., Wenger, L. M., Gross, O. P., & Harrison, S. C. (2002). Hydrocarbon systems analysis of the northern Gulf of Mexico: Delineation of hydrocarbon migration pathways using seeps and seismic imaging. *Surface exploration case histories: Applications of geochemistry, magnetics, and remote sensing: AAPG Studies in Geology*, *48*, 25–40.

Hunt, A. G., Darrah, T. H., & Poreda, R. J. (2012). Determining the source and genetic fingerprint of natural gases using noble gas geochemistry: A northern Appalachian Basin case study. *AAPG Bulletin*, *96*(10), 1785–1811.

Kharaka, Y. K., & Specht, D. J. (1988). The solubility of noble gases in crude oil at 25–100 C. *Applied Geochemistry*, *3*(2), 137–144.

Kipfer, R., Aeschbach-Hertig, W., Peeters, F., & Stute, M. (2002). Noble gases in lakes and ground waters. *Reviews in Mineralogy and Geochemistry*, *47*(1), 615–700.

Lawson, M., Formolo, M. J., Summa, L., & Eiler, J. M. (2018). Geochemical applications in petroleum systems analysis: New constraints and the power of integration. *Geological Society, London, Special Publications*, *468*, SP468–SP466. https://doi.org/10.1144/SP468.6

Lee, J. Y., Marti, K., Severinghaus, J. P., Kawamura, K., Yoo, H. S., Lee, J. B., & Kim, J. S. (2006). A redetermination of the isotopic abundances of atmospheric Ar. *Geochimica et Cosmochimica Acta*, *70*(17), 4507–4512.

Lowenstern, J. B., Evans, W. C., Bergfeld, D., & Hunt, A. G. (2014). Prodigious degassing of a billion years of accumulated radiogenic helium at Yellowstone. *Nature*, *506*(7488), 355–358.

Moyer, M. C., Barry, M. D., & Tears, N. C. (2001). Hoover-Diana deepwater drilling and completions: Proceedings Offshore Technology Conference, Houston, OTC 13081, 19 p.

Pepin, R. O. (2000). On the isotopic composition of primordial xenon in terrestrial planet atmospheres. In *From dust to terrestrial planets* (pp. 371–395). Netherlands: Springer.

Pinti, D. L., & Marty, B. (1995). Noble gases in crude oils from the Paris Basin, France: Implications for the origin of fluids and constraints on oil–water-gas interactions. *Geochimica et Cosmochimica Acta*, *59*(16), 3389–3404.

Pitre, F., & Pinti, D. L. (2010). Noble gas enrichments in porewater of estuarine sediments and their effect on the estimation of net denitrification rates. *Geochimica et Cosmochimica Acta*, *74*(2), 531–539.

Podosek, F. A., Bernatowicz, T. J., & Kramer, F. E. (1981). Adsorption of xenon and krypton on shales. *Geochimica et Cosmochimica Acta*, *45*(12), 2401–2415.

Pourciau, R. D., Fisk, J. H., Descant, F. J., & Waltman, R. B. (2003, January). Completion and well performance results, Genesis Field, deepwater Gulf of Mexico. In SPE Annual Technical Conference and Exhibition. Society of Petroleum Engineers.

Prinzhofer, A. (2013). Noble gases in oil and gas accumulations. In *The noble gases as geochemical tracers* (pp. 225–247). Berlin: Springer.

Rafalowski, J. W., Regel, B. W., Jordan, D. L., & Lucidi, D. O. (1994). Green Canyon Block 205 lithofacies, seismic facies and reservoir architecture. In P. Weimer, A. Bouma, & B. Perkins, (Eds.), *Submarine fans and turbidite systems, sequence stratigraphy, reservoir architecture and production characteristics: Gulf Coast Section SEPM 15th Annual Research Conference* (pp. 293–305).

Rowan, M. G., & Weimer, P. (1998). Salt-sediment interaction, northern Green Canyon and Ewing bank (offshore Louisiana), northern Gulf of Mexico. *AAPG Bulletin*, *82*(5), 1055–1082.

Sales, J. K. (1997). AAPG Memoir 67: Seals, traps, and the petroleum system. Chapter 5: Seal Strength vs. Trap Closure--A Fundamental Control on the Distribution of Oil and Gas.

Sano, Y., Wakita, H., & Sheng, X. (1988). Atmospheric helium isotope ratio. *Geochemical Journal*, *22*(4), 177–181.

Seldon, B., & Flemings, P. B. (2005). Reservoir pressure and seafloor venting: Predicting trap integrity in a Gulf of Mexico deepwater turbidite minibasin. *AAPG Bulletin*, *89*(2), 193–209.

Smith, S. P. (1985). Noble gas solubility in water at high temperature. *Eos*, *66*, 397.

Smith, S. P., & Kennedy, B. M. (1983). The solubility of noble gases in water and in NaCl brine. *Geochimica et Cosmochimica Acta*, *47*, 503–515. https://doi.org/10.1016/0016-7037(83)90273-9

Solomon, D. K., Hunt, A., & Poreda, R. J. (1996). Source of radiogenic helium 4 in shallow aquifers: Implications for dating young groundwater. *Water Resources Research*, *32*, 1805–1813. https://doi.org/10.1029/96WR00600

Stolper, D. A., Lawson, M., Formolo, M. J., Davis, C. L., Douglas, P. M., & Eiler, J. M. (2018). The utility of methane clumped isotopes to constrain the origins of methane in natural gas accumulations. *Geological Society, London, Special Publications*, *468*(1), 23–52.

Sullivan, M., & Templet, P. (2002). Characterization of fine-grained deep-water turbidite reservoirs: Examples from Diana Sub-basin, western Gulf of Mexico. In P. Weimer, M. Sweet, M. Sullivan, J. Kendrick, D. Pyles, & A. Donovan (Eds.), *Deep-water core workshop, Northern Gulf of Mexico: GCSSEPM Foundation* (pp. 75–92).

Sweet, M. L., & Sumpter, L. T. (2007). Genesis field, Gulf of Mexico: Recognizing reservoir compartments on geologic and production time scales in deep-water reservoirs. *AAPG Bulletin*, *91*(12), 1701–1729.

Tolstikhin, I., Kamensky, I., Tarakanov, S., Kramers, J., Pekala, M., Skiba, V., et al. (2010). Noble gas isotope sites and mobility in mafic rocks and olivine. *Geochimica et Cosmochimica Acta*, *74*(4), 1436–1447.

Tolstikhin, I., Lehmann, B. E., Loosli, H. H., & Gautschi, A. (1996). Helium and argon isotopes in rocks, minerals, and related ground waters: A case study in northern Switzerland. *Geochimica et Cosmochimica Acta*, *60*(9), 1497–1514.

Tolstikhin, I. N., Ballentine, C. J., Polyak, B. G., Prasolov, E. M., & Kikvadze, O. E. (2017). The noble gas isotope record of hydrocarbon field formation time scales. *Chemical Geology*, *471*, 141–152.

Torgersen, T. (2010). Continental degassing flux of ^{4}He and its variability. *Geochemistry, Geophysics, Geosystems*, *11*, Q06002. https://doi.org/10.1029/2009GC002930

Torgersen, T., & Clarke, W. B. (1985). Helium accumulation in groundwater, I: An evaluation of sources and the continental flux of crustal ^{4}He in the Great Artesian Basin, Australia. *Geochimica et Cosmochimica Acta*, *49*(5), 1211–1218.

Torgersen, T., & Ivey, G. N. (1985). Helium accumulation in groundwater. II: A model for the accumulation of the crustal 4 He degassing flux. *Geochimica et Cosmochimica Acta*, *49*(11), 2445–2452.

Torgersen, T., & Kennedy, B. M. (1999). Air-Xe enrichments in Elk Hills oil field gases: role of water in migration and storage. *Earth and Planetary Science Letters*, *167*(3), 239–253.

Warr, O., Lollar, B. S., Fellowes, J., Sutcliffe, C. N., McDermott, J. M., Holland, G., et al. (2018). Tracing ancient hydrogeological fracture network age and compartmentalisation using noble gases. *Geochimica et Cosmochimica Acta*, *222*, 340–362.

Zartman, R. E., Wasserburg, G. J., & Reynolds, J. H. (1961). Helium, argon, and carbon in some natural gases. *Journal of Geophysical Research*, *66*, 277–306. https://doi.org/10.1029/Jz066i001p00277

Zhou, Z., & Ballentine, C. J. (2006). 4 He dating of groundwater associated with hydrocarbon reservoirs. *Chemical Geology*, *226*(3), 309–327.

Zhou, Z., Ballentine, C. J., Kipfer, R., Schoell, M., & Thibodeaux, S. (2005). Noble gas tracing of groundwater/coalbed methane interaction in the San Juan Basin, USA. *Geochimica et Cosmochimica Acta*, *69*(23), 5413–5428.

Zhou, Z., Ballentine, C. J., Schoell, M., & Stevens, S. H. (2012). Identifying and quantifying natural CO_2 sequestration processes over geological timescales: The Jackson Dome CO_2 Deposit, USA. *Geochimica et Cosmochimica Acta*, *86*, 257–275.